Supporting Information

NO_2 and SO_2 Adsorption and Sensing on Janus B_2SeTe: Unveiling Its Electronic, Optical, and Magnetic Properties Using DFT and COMSOL

Manik Bala, Md Tawabur Rahman*, Raiyan Al Nahean, and Md Sakib Hasan Khan

Department of Electrical and Electronic Engineering, Khulna University of Engineering & Technology, Khulna-9203, Bangladesh

*Corresponding Author: tawabur@eee.kuet.ac.bd

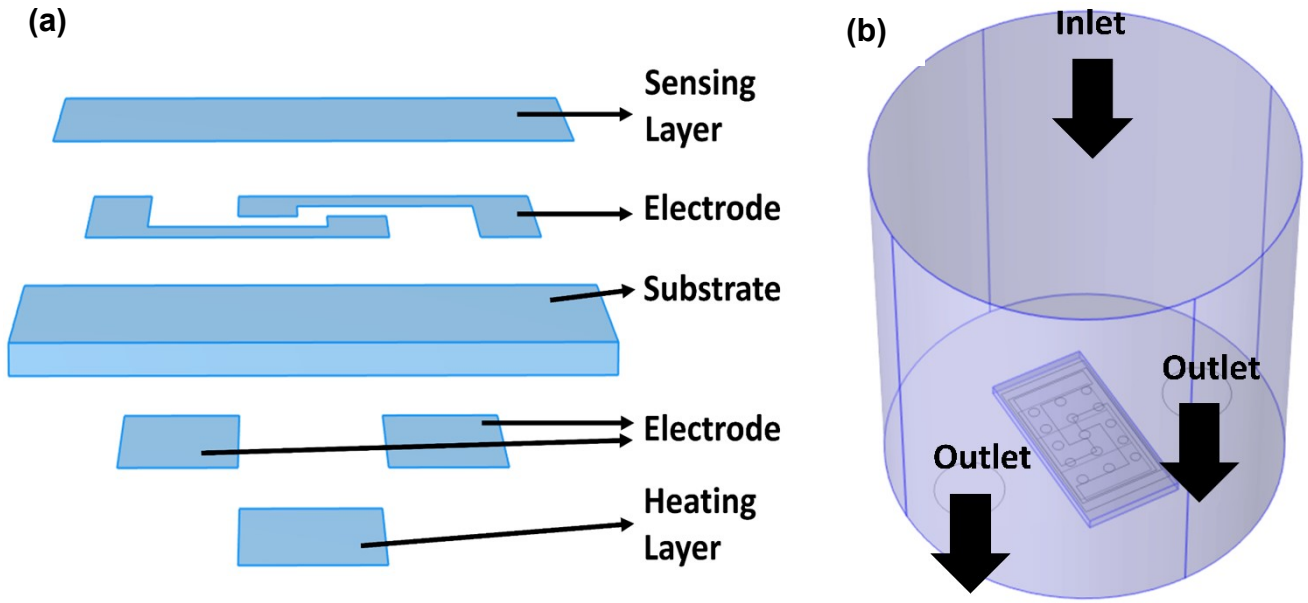

Fig. S1 (a) Sensor structure in COMSOL represents different layers of the proposed gas sensor. (b) Gas chamber model housing the sensor with a gas inlet and two outlets.

Table S I The lattice constant a; bond lengths of B-Se (d1), B-B (d2) and B-Te (d3); bond angles of B-B-Se (θ1), B-B-Te (θ2), B-Se-B(θ3) and B-Te-B (θ4); the thickness layer(t); the work function (Φ); the band gap (E_g); VBM/CBM positions.

a(Å)	d1(Å) d2(Å) d3(Å)	t(Å)	θ1(°) θ2(°) θ3(°) θ4(°)	Φ(eV)	E_g(eV)	Stability	VBM/CBM positions
4.07	2.153 1.683 2.129	4.9	114.329 117.871 104.215 99.914	5.307	2.151	Dynamically Stable	Γ- M

(a) NO_2+CO_2

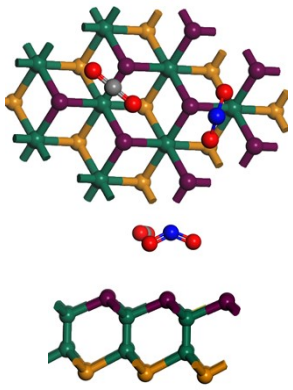

(b) NO_2+CO

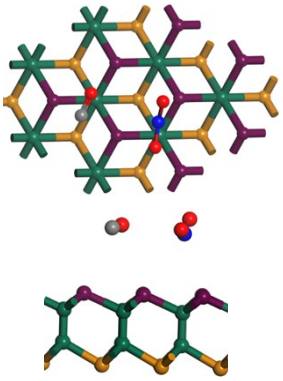

(c) NO_2+CO_2+NH

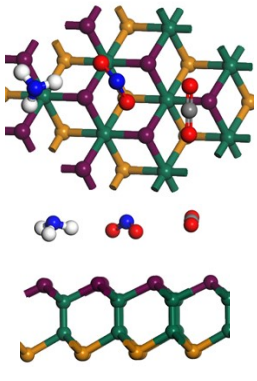

(d) NO_2+CO+CH_4

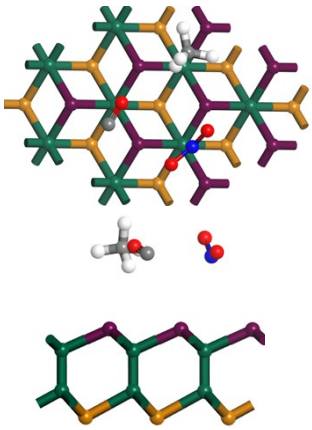

(e) CO_2+HCN+H_2S

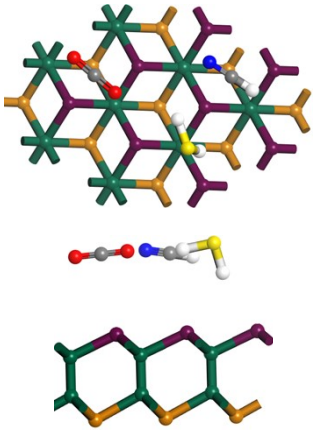

(f) H_2S+HCN+NH_3

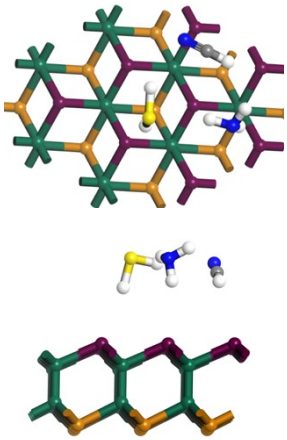

(g) SO_2+H_2S+NH_3

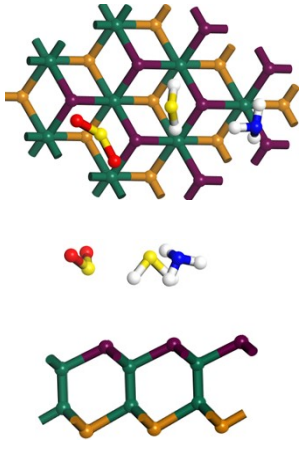

(h) CO+CH_4+NH_3

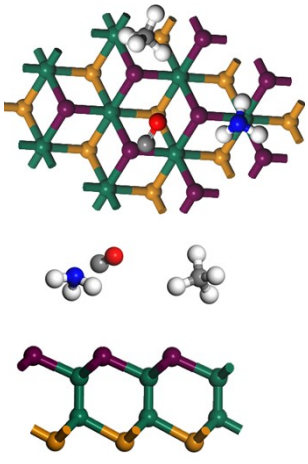

(i) NH_3+CO+CH_4+H_2S

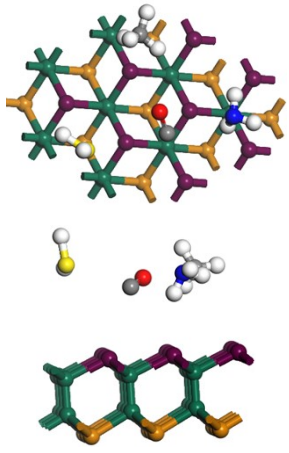

N O C H S B Se T

Fig. S2 Top and side view of the most energetically favourable adsorption configuration of the adsorbed molecules (a) NO_2+CO_2, (b) NO_2+CO, (c) NO_2+CO+CH_4, (d) NO_2+CO_2+NH_3, (e) CO_2+HCN+H_2S, (f) H_2S+ HCN+NH_3, (g)SO_2+ H_2S+NH_3, (h) CO+CH_4+NH_3, and (i) NH_3+CO+CH_4+H_2S molecules on the B_2SeTe monolayer.

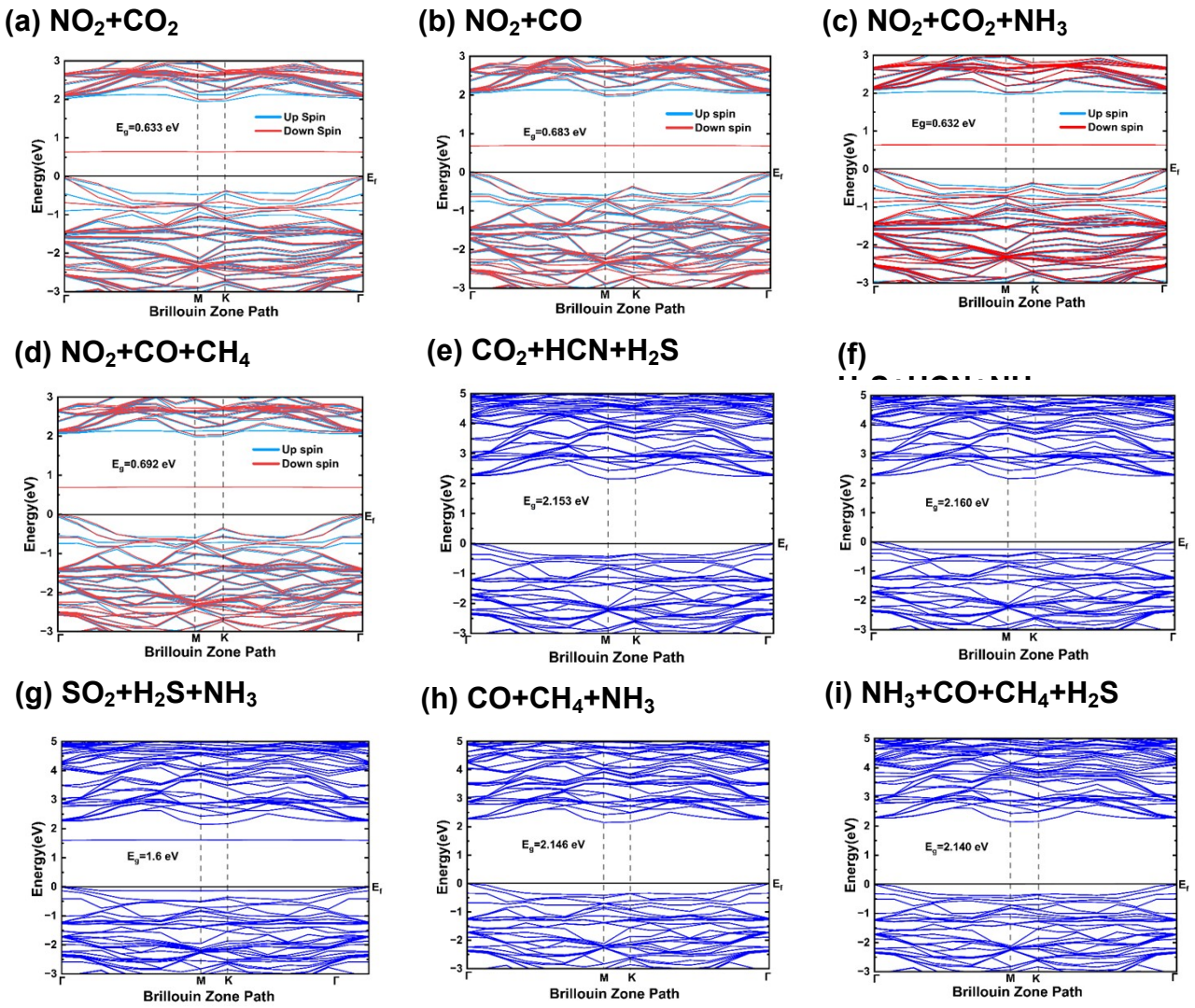

Fig. S3 The band structures (a) NO_2+CO_2, (b) NO_2+CO, (c) NO_2+CO+CH_4, (d) NO_2+CO_2+NH_3, (e) CO_2+HCN+H_2S, (f) H_2S+HCN+NH_3, (g) SO_2+H_2S+NH_3, (h) CO+CH_4+NH_3, and (i) NH_3+CO+CH_4+H_2S adsorbed B_2SeTe monolayer. The blue (red) colour indicates up (down) spin. Due to the presence of NO_2 gas, the bandgap changes rustically from the pristine value of 2.151 eV. In the absence of NO_2 gas, other gas-adsorbed structures have a band gap reasonably similar to the pristine band gap value.

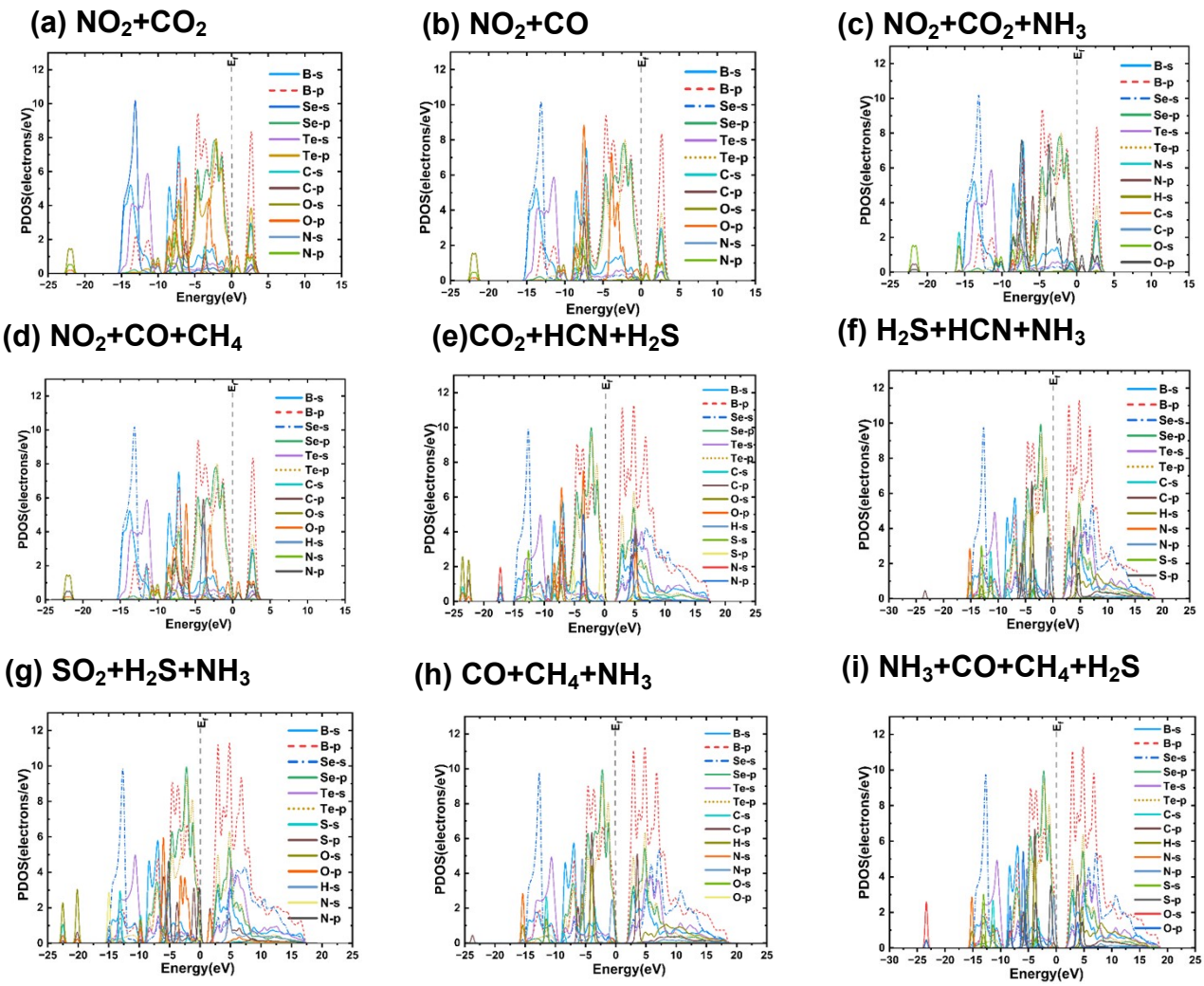

Fig. S4 The orbital projected density of states of (a) NO_2+CO_2, (b) NO_2+CO, (c) NO_2+CO+CH_4, (d) NO_2+CO_2+NH_3,(e) CO_2+HCN+H_2S, (f) H_2S+HCN+NH_3, (g)SO_2+H_2S+NH_3, (h) CO+CH_4+NH_3, and (i) NH_3+CO+CH_4+H_2S absorbed B_2SeTe monolayer. Due to the presence of NO_2 gas, the bandgap changes rustically from the pristine value of 2.151 eV. In the absence of NO_2 gas, other gas-adsorbed structures have a band gap reasonably similar to the pristine band gap value.

Table S II Band gap, change in band gap, sensitivity, and logarithmic sensitivity for different gas combinations.

Adsorbed gas	Bandgap (E_g)	Change in bandgap (ΔE_g)	Sensitivity (%S)	Log_{10} (S%)
NH_3	2.153	0.002	3.8	0.58
HCN	2.156	0.005	9.209	0.97
CO	2.154	0.003	86.335	1.93
NO_2	0.538	-1.613	3.4401×10^{15}	13.53
SO_2	1.275	-0.876	2.2466×10^{9}	7.35
CO_2	2.164	0.013	22.22	1.34
H_2S	2.166	0.015	25.162	1.4
CH_4	2.154	0.003	5.6322	0.74
NO_2+CO_2	0.633	-1.518	5.486×10^{14}	14.74
NO_2+CO	0.683	-1.468	2.087×10^{14}	14.32
NO_2+CO_2+NH_3	0.632	-1.519	5.6×10^{14}	14.74
NO_2+CO+CH_4	0.692	-1.459	1.75×10^{14}	14.24
CO_2+HCN+H_2S	2.153	0.002	3.8	0.58
H_2S+HCN+NH_3	2.160	0.009	15.96	1.20
SO_2+H_2S+NH_3	1.6	-0.551	4.2×10^{6}	6.623
CO+CH_4+NH_3	2.146	-0.005	10.14	1
NH_3+CO+CH_4+H_2S	2.140	-0.011	23.68	1.37

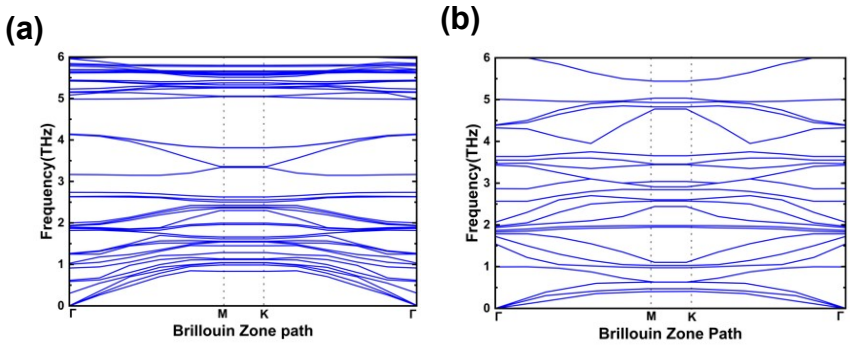

Fig. S5 Phonon dispersion curves of (a) NO_2 and (b) SO_2 adsorbed on B_2SeTe monolayer